PAPER

A didactic proposal about Rutherford backscattering spectrometry with theoretic, experimental, simulation and application activities

To cite this article: Federico Corni and Marisa Michelini 2018 *Eur. J. Phys.* **39** 015501

View the article online for updates and enhancements.

A didactic proposal about Rutherford backscattering spectrometry with theoretic, experimental, simulation and application activities

Federico Corni[1,3] and **Marisa Michelini**[2]

[1] Department of Education and Humanities, University of Modena and Reggio Emilia, Via A. Allegri, 9-42121 Reggio Emilia, Italy
[2] Dipartimento di Chimica, Fisica e Ambiente, University of Udine, Via delle Scienze 206-33100 Udine, Italy

E-mail: federico.corni@unimore.it and marisa.michelini@uniud.it

Abstract

Rutherford backscattering spectrometry is a nuclear analysis technique widely used for materials science investigation. Despite the strict technical requirements to perform the data acquisition, the interpretation of a spectrum is within the reach of general physics students. The main phenomena occurring during a collision between helium ions—with energy of a few MeV—and matter are: elastic nuclear collision, elastic scattering, and, in the case of non-surface collision, ion stopping. To interpret these phenomena, we use classical physics models: material point elastic collision, unscreened Coulomb scattering, and inelastic energy loss of ions with electrons, respectively. We present the educational proposal for Rutherford backscattering spectrometry, within the framework of the model of educational reconstruction, following a rationale that links basic physics concepts with quantities for spectra analysis. This contribution offers the opportunity to design didactic specific interventions suitable for undergraduate and secondary school students.

Supplementary material for this article is available online

Keywords: Rutherford backscattering spectrometry, (RBS), scattering cross-section, simulation

(Some figures may appear in colour only in the online journal)

---

[3] Author to whom any correspondence should be addressed.

1. Introduction

Modern physics has been introduced in the curricula of all European countries, starting from secondary school level. Besides teaching the new theories of quantum mechanics, as well as the issues on which they are based, a complementary contribution consists of giving students the opportunity to experience how researchers work in applied research labs and, in particular, how basic physics concepts ground the analysis techniques. It is important for students to learn that in physics the discovery and understanding of a phenomenon often lead to the development of new applications and analysis techniques, which open novel technological/research fields and allow measurements never possible before.

Rutherford backscattering spectrometry (RBS) (Chu *et al* 1978, Feldman and Mayer 1986), chronologically the first of the ion beam analysis (IBA) techniques developed in the early 20th century, is based on the famous Rutherford experiment (Rutherford 1911, 2012). An RBS measurement consists of sending a monoenergetic, collimated, light ion beam (typically H^+ or He^{++}) towards the surface of a sample, and in the collection of the energy spectrum of the ions of the beam which, after a collision with the target atoms, are backscattered along a certain direction into the active area of a solid-state detector. After RBS, other IBA techniques have been developed according to the various phenomena occurring in ion-matter interactions[4]: Particle-induced x-ray emission (Chadwick 1913), where the x-ray emitted by the target atoms is analyzed, elastic non-Rutherford backscattering spectrometry (Chadwick and Bieler 1921), where the ion energy allows the target atom Coulomb barrier to be exceeded, and nuclear reaction analysis (Rutherford and Chadwick 1922), where nuclear reactions are caused between ions and target atoms. The great virtue of RBS among IBA techniques is its simplicity, which has enabled its establishment as a primary reference method for non-destructive materials science analyses (Jeynes 2017) in electronics, chemistry, earth science, works of art, and, in general, in applied sciences.

It is its very simplicity that makes RBS pedagogically attractive, because it is a modern physics technique with results that are interpreted by means of classical physics concepts, without the need of quantum mechanics knowledge. According with our experience (Michelini and Santi 2008, Corni 2008, 2010, Michelini 2010b, Mossenta 2010, 2012, Battaglia *et al* 2011), RBS can be integrated in university general physics courses as well as in the secondary school curriculum in its vertical development, allowing students to understand the role of conservation principles and of fundamental quantities, e.g. cross-section, in theory and in applications.

Although many physics education contributions concern the Rutherford experiment and the scattering cross-section, either theoretically (Chong and Andrews 1993, Gauthier 2000), or experimentally (Wicher 1965, Lee *et al* 1968, Eaton and Cheetham 1973, Grober *et al* 2010), RBS is completely ignored.

In this paper, within the theoretical framework of the model of educational reconstruction (Duit *et al* 2005) and by means of the Design-Based Research (DBR 2003, Lijnse 1995), intervention modules are carried out to develop and test research-based learning proposals (Anderson and Shattuck 2012) for vertical teaching-learning paths based on experimental work (Michelini 2010a, Michelini *et al* 2016).

We will present the educational proposal for RBS organized in terms of key questions to offer the teacher the opportunity to structure didactic specific interventions suitable for every context. We follow a rationale (table 1) linking basic physics concepts (table 1, first column) with quantities for spectra analysis (table 1, second column).

---

[4] For a historical and complete review of IBA techniques, see (Chris Jeynes and Colaux 2016).

Table 1. Rationale of the RBS proposal.

Basic physics concepts	Correlated quantities for spectra analysis
Ion-nucleus collision	**Kinematic factor**
• material point elastic collision	• information about the energy of a back-scattered ion
• conservation of energy and momentum	• identification of the elements at the sample surface
Ion Coulomb scattering	**Scattering cross-section**
• charged particle scattering by a target nucleus	• information about the collision probability between an ion and a target nucleus
• conservative central force: conservation of energy and angular momentum	• information about the spectrum yield of a film of a pure element
• impulse theorem	• evaluation of the atomic fractions of the elements present in a compound film
Ion inelastic stopping	**Stopping cross-section**
• charged particle-electron inelastic collisions	• Information about the ion stopping power of an element's atoms
• energy loss	• Evaluation of thicknesses of films and of depth distribution of elements

2. What is RBS?

Although RBS measurements require large facilities to get the spectra (a MeV ion accelerator to produce the probe beam, vacuum lines to manage and transport the beam, a sample vacuum chamber where the collision between the beam and the sample occurs, and electronic data acquisition systems to detect and analyze the signals), RBS analysis is within the reach of everyone, because of the simplicity of the underlying concepts.

RBS spectra provide information about mass and depth distribution of the constituent elements in the first few hundred nanometers of a sample surface. Under certain conditions of beam and sample alignment, channeling-RBS (Feldman and Mayer 1982) spectra also provide information about the crystal order, kind of defects and damage profile in crystalline samples. With the geometrical setup (grazing incidence and detection angles) allowing the detection of recoiling target atoms in the forward direction, light-element profiling is performed with forward recoil spectrometry (Feldman and Mayer 1986). In this paper, we will focus specifically on conventional RBS.

An RBS spectrum of a compound layered sample can be roughly seen as the superposition of the spectra of the single composing elements, weighted by the composition fraction, and displaced in energy according to the distance from the surface.

Figure 1 shows a typical RBS spectrum. The vertical axis shows the RBS yield, i.e. the fraction of backscattered ions normalized to the detector solid angle and to the energy
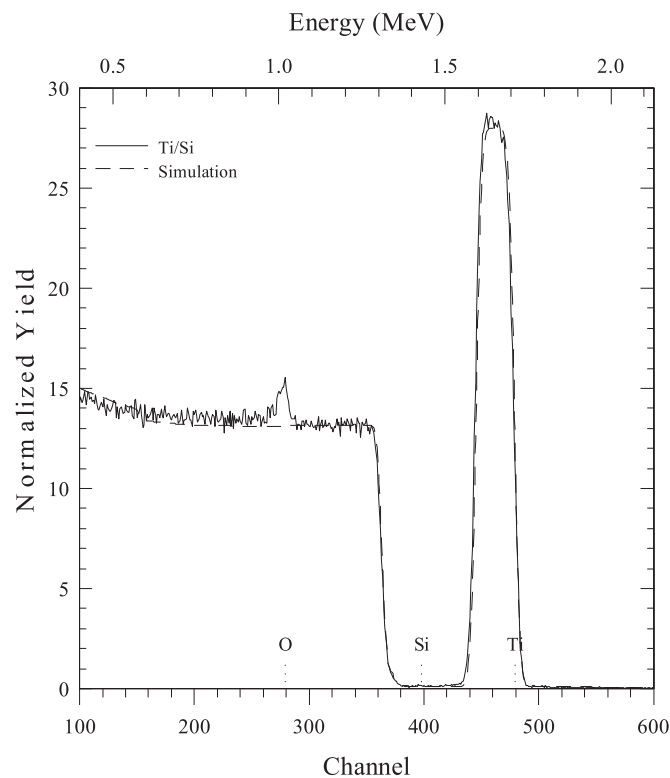
Figure 1. RBS spectrum (solid line) and simulation (dashed line) of a layer of 100 nm of Ti (peak at high energy) on a Si substrate (large band towards low energies), with a small contamination of oxygen (peak at about 1 MeV). Parameters of the measurement: beam energy 2.2 MeV, scattering angle 120°.

calibration factor[5]. The bottom axis reports the channel number coming from the multi-channel analyzer, the top axis the ion energy, resulting after the channel-energy calibration. The expected energy edges of oxygen, silicon and titanium at the surface are marked.

2.1. The features of RBS

From a didactic point of view, it is important that the students discuss the feature of RBS allowing the use of classical physics models, i.e. material point elastic collision, unscreened Coulomb scattering, and inelastic energy loss of ions with electrons.

2.1.1. Elastic collision. High-energy beam allows the interaction of the backscattered ion with matter to be considered as an elastic collision with an unscreened target atom nucleus. This condition avoids electron interaction that would cause energy loss.

The students easily evaluate the needed beam energy by imposing that the closest distance r reachable by a He ion of energy E in a head-on collision with an unscreened nucleus of a generic element of atomic number Z is smaller than the Bohr radius r_B of a single

---

[5] Ion energy calibration (the linear relation between the channel number and the ion energy—the calibration factor being the slope of this straight line) results from the analysis of RBS spectra of reference samples with known structure and composition.

electron ion of the element:

$$r = \frac{1}{4\pi\epsilon_0} \frac{2Ze^2}{E} < \frac{a_0}{Z} = r_{\mathrm{B}} \qquad (1)$$

where a_0 is the Bohr radius of hydrogen. The minimum energy results in $54Z^2$ in eV units, i.e. about 10 keV for Si, 330 keV for Au, and, however less than 1 MeV even for the heaviest target elements. Conventional RBS employs He ion beams of about 2 MeV.

2.1.2. Light ions. The use of light ions such as H^+ or He^{++}, or any with masses lower than those of the target atoms, makes the backscattering possible. In contrast, the ion would be scattered in the forward direction and lost into the material. Students verify this condition by studying the equations resulting from an activity in section 3.1.

2.1.3. Single scattering. In the case of non-surface scattering, ions lose energy in their inward and outward paths. Energy loss can be due to interactions with electrons and with nuclei.

Multiple scattering, in addition to that with the target nucleus, happens in particular for heavy elements and results in a lower energy of the emerging ion than that expected for a single scattering. By neglecting the low-energy part of an RBS spectrum, multiple scattering events and superimposition of signals are excluded.

Energy loss is then only due to electrons. For the very large number and very light mass of electrons, the loss is the result of numerous small losses that can be treated statistically and be thought of as a sort of uniform friction.

3. Inquiry-based approach to RBS

According to our experimental approach, the educational treatment of RBS follows a sequence of inquiry-type questions, to prepare a problem-solving activity. We are interested in obtaining information about the sample composition and structure from the spectra. First, we will focus on the particular case of surface elements (sections 3.1–3.2), then we will consider the more general case of elements buried in the first few hundred nanometers from the surface (section 3.3). For every topic, we supply experimented didactic activities (Michelini and Santi 2008, Corni 2008, 2010, Michelini 2010b, Mossenta 2010, 2012, Battaglia *et al* 2011) suitable for all kinds of student inclination and laboratory equipment: from theoretic calculation to experimental investigation, from computer simulation to application for materials analysis. We divide them into introductory activities (sections 3.1–3.3)—some of them inspired by the literature—about the single phenomenon of RBS, and advanced activities (section 3.4) about the RBS technique itself. Some introductory activities will concern macroscopic simulators of the atomic phenomena occurring in RBS, so the dependence of the various quantities on atomic number will disappear.

3.1. Atomic masses of the target atoms and the elastic nuclear collision

We are interested in identifying the elements present on the sample surface, i.e. in evaluating their atomic masses. The energy fractions of two material points after an elastic collision depends only on their masses, for a given scattering angle. By imposing the conservation of energy and momentum, and defining the kinematic factor $K(M, \theta)$ as the ratio between the ion energy after, $E(M, \theta)$, and before, E_0, the collision, we calculate the energy of an ion backscattered at angle θ as a function of the mass M of the target element.

Note that the calculation of the kinematic factor does not depend on the kind of inter-action, i.e. the (conservative) force responsible for the scattering.

3.1.1. Didactic activity: calculation of the kinematic factor (introductory—student exercise). By solving the conservation equations of (bi-dimensional) momentum and of kinetic energy of an impinging ion of mass m and energy $E_0 = \frac{1}{2}mv_0^2$ with a target atom of mass M initially at rest

$$\begin{cases} \frac{1}{2}mv_0^2 = \frac{1}{2}mv^2 + \frac{1}{2}MV^2 \\ mv_0 = mv \cos\theta + MV \cos\phi \\ 0 = mv \sin\theta - MV \sin\phi \end{cases} \tag{2}$$

where ϕ is the recoil scattering angle, we calculate the kinematic factor:

$$K(M, \theta) = \frac{E}{E_0} = \left(\frac{\sqrt{M^2 - m^2 \sin^2\theta} + m \cos\theta}{M + m} \right)^2. \tag{3}$$

By studying this equation, we notice that the scattering angle allows the best mass resolution, i.e. the geometrical condition that produces the maximum change in $K(M, \theta)$ with a given (small) variation of M, is $\theta \to \pi$, i.e. just the backscattering condition.

3.1.2. Didactic activity: measurement of the kinematic factor (introductory—experimental). The kinematic factor, in the case of head-on collision $\theta = \pi$, can be experimentally evaluated in the didactic laboratory using a macroscopic simulator with track and carts. A cart of known mass m, representing the ion, is sent towards a second cart with mass $M > m$ initially at rest, representing the target atom, the two carts being equipped with spring bumpers. By means of sonar sensor measurements, the velocity of the first cart just before and after the collision is measured from the slope of position versus time graph. By varying M, the experimental kinematic factor as a function of m/M is obtained. Figure 2 shows the data compared to the theoretical expectation given by equation (3).

3.2. Fraction of an element and the unscreened Coulomb scattering

Once we have identified, by their energy, the backscattered ions coming from the atoms of a given element, we are interested in quantifying the surface fraction of this element. It is a statistical problem and for this, different from many textbooks that reduce the treatment to only geometrical considerations, it is important from an educational point of view (Corni *et al* 1996). We think in terms of RBS normalized yield $Y(\theta) = \frac{N(\theta)}{N_{tot}} \frac{1}{\Omega}$, i.e. number of detected ions $N(\theta)$ backscattered by the element atoms within a solid angle Ω around θ with respect to the total number of sent ions N_{tot}[6]: this fraction is related to the number of atoms of the element per unit area and is strongly dependent on their atomic number. We have to calculate the probability $P(\theta)$ of scattering: in this case, we need to know the form of the ion-nucleus interaction, which determines the spreading of ion trajectories.

If we define the scattering cross-section $\sigma(Z, \theta)$ of an element of atomic number Z as this probability $P(\theta)$ per unit solid angle for one atom of the element per unit area:

$$\sigma(Z, \theta) = P(\theta) \frac{1}{\Omega} \frac{1}{n} \tag{4}$$

---

[6] The energy calibration factor, introduced in section 2, comes from numerical computation, here ignored for theoretical treatment.
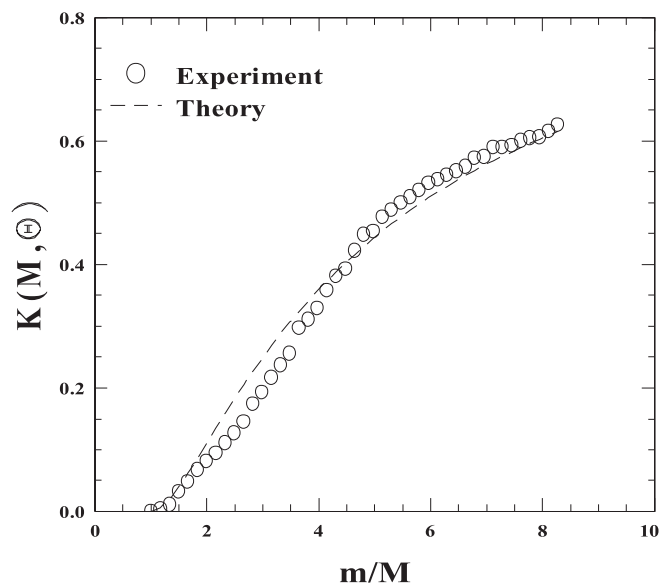
Figure 2. Experimental values of the kinematic factor using track and carts (m = 0.605 kg, 0.605 kg $\leqslant$ M $\leqslant$ 5.008 kg) compared to the theoretical expectation (equation (3)).

where n is the number of atoms per unit area, we calculate it theoretically by knowing the way ion trajectories are bent by the unscreened nucleus Coulomb force. The scattering cross-section is strongly dependent on the atomic number of the element, besides the scattering angle. Approximating probability with frequency, we then can evaluate the element surface density n through the experimental RBS normalized yield:

$$n = \frac{Y(\theta)}{\sigma(Z, \theta)}. \tag{5}$$

3.2.1. Didactic activity: calculation of the Rutherford scattering cross-section (introductory—student exercise). The theoretical calculation of the scattering cross-section $\sigma(Z, \theta)$ of an element of atomic number Z requires the expression of $P(\theta)$. We profit from the cylindrical symmetry and introduce the impact parameter $b(Z, \theta)$, as the distance between the ion original direction and the target nucleus (figure 3). If we consider one target atom in a unit surface, the ions collected in a solid angle $\Omega = 2\pi \sin \theta d\theta$ are those coming from a ring area of radius $b(Z, \theta)$ and thickness db, i.e. $2\pi b(Z, \theta) db$, where the relation between θ and $b(Z, \theta)$ is defined by the form of the interaction force. If S is the beam section area, D is the beam current section density, and t the measurement time interval, $2\pi b(Z, \theta) db Dt$ is the charge that will be collected after the scattering and SDt the total charge sent. Then:

$$\sigma(Z, \theta) = -\frac{2\pi b(Z, \theta) db\, Dt}{SDt} \frac{1}{2\pi \sin \theta d\theta} \frac{1}{n} = -\frac{b(Z, \theta)}{\sin \theta} \frac{db}{dt} \tag{6}$$

where we have set $n = 1$ and $S = 1$. The minus sign means that $b(Z, \theta)$ decreases with increasing θ.

Equation (6) shows that the calculation of the scattering cross-section is a matter of finding the relation between the scattering angle and the impact parameter and of computing
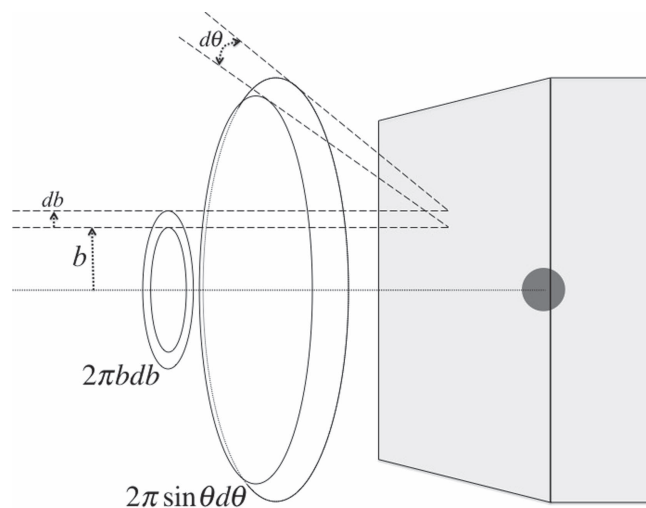
Figure 3. Geometrical illustration of the quantities used to calculate the scattering cross-section in equation (6).

the derivative of $b(Z, \theta)$ with respect to θ. By assuming the target atom at rest (i.e. no energy exchange during the collision), this calculation for He^{++} ions proves to be particularly simple, though introducing a small error[7] with respect to the more general case of the recoiling target atom:

$$b(Z, \theta) = \frac{Ze^2}{E_0} \tan^{-1} \frac{\theta}{2} \tag{7}$$

and

$$\sigma(Z, \theta) = -\frac{b(Z, \theta)}{\sin \theta} \frac{db}{dt} = \left(\frac{Ze^2}{2E_0}\right)^2 \sin^{-4} \frac{\theta}{2}, \tag{8}$$

which is the well-known formula of the Rutherford backscattering cross-section. Hints for the calculation of equation (7) are in (Chu *et al* 1978).

3.2.2. Didactic activity: calculation of the hard-sphere scattering cross-section of a circular-shaped planar target (introductory—student exercise). To give concreteness to this concept, students can be involved in the calculation of the scattering cross-section in the case of 2D elastic hard-sphere collision with forms of geometrical shapes. Equation (6), in a plane, reduces to $\sigma(\theta) = -\frac{db}{dt}$. In the case of a circular form, from figure 4 (top), we find $b(\theta) = R \cos \frac{\theta}{2}$, and

$$\sigma(\theta) = \frac{R}{2} \sin \frac{\theta}{2}. \tag{9}$$

3.2.3. Didactic activity: calculation of the shape of a planar form leading to the 2D Rutherford cross-section in the case of hard-sphere scattering (introductory—student exercise). Recalling equation (7) and with reference to figure 4 (bottom), the slope of the tangent to

---

[7] The error increases with decreasing mass, e.g. 0.08% for Au and 6% for Na.
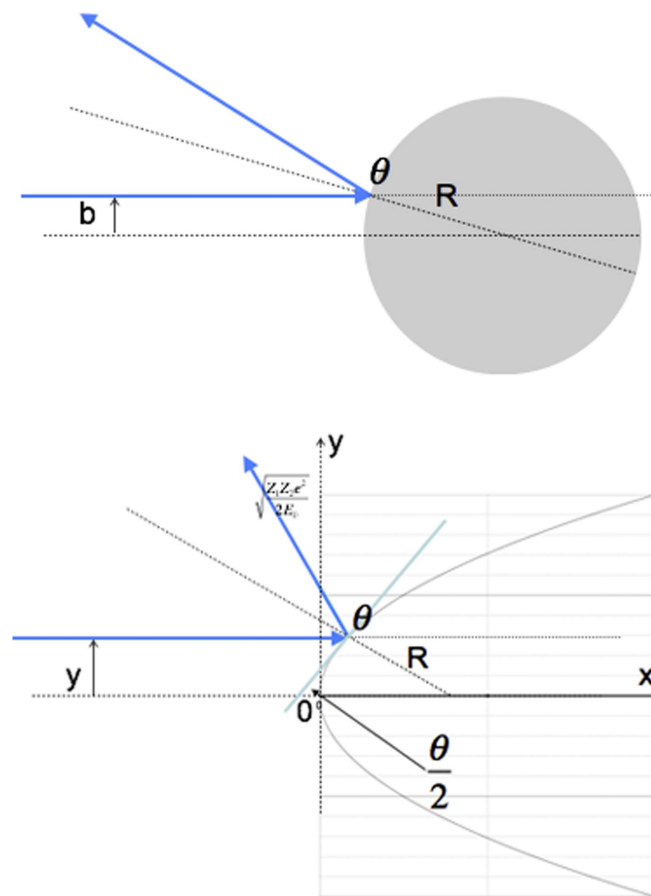
Figure 4. (top) Geometry leading to equation (9). (bottom) Geometrical construction of the shape of a planar target leading to the 2D Rutherford cross-section in the case of hard-sphere scattering.

the shape in the collision point is $\frac{dy}{dx} = \tan\frac{\theta}{2} = \frac{\left(\frac{Ze^2}{2E_0}\right)}{y}$ leading to the equation for the form shape:

$$y = \sqrt{\frac{Ze^2}{E_0}x}, \tag{10}$$

which is a parabola with $y = 0$ symmetry axis.

3.2.4. Didactic activity: measurement of the hard-sphere scattering cross-section of a circular-shaped planar form (introductory—experimental). This activity, employing a macroscopic simulator, allows the students, perhaps for the first time, to be involved in and to reflect on the statistical character of the cross-section and about the quantities to be introduced into the equations, such as Ω and n.

    The measurement of the scattering cross-section in the case of 2D hard-sphere collision can be performed using a glass marble and a wooden circular form. The marble is repeatedly launched along parallel, equally spaced, directions towards the form using a launch guide
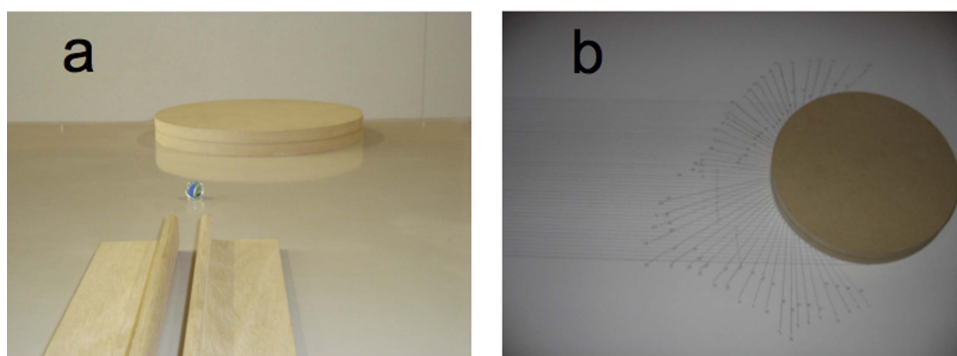
Figure 5. (a) Launch guide and circular wooden form for marble collision. (b) Tracking of the marble trajectories.
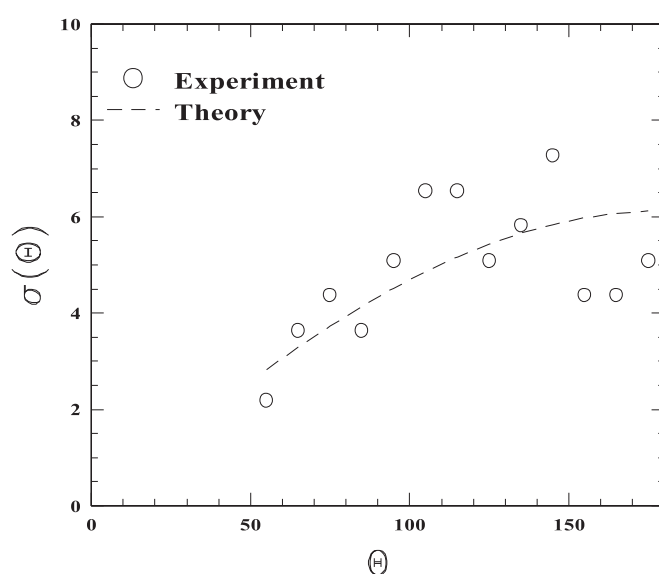

Figure 6. Measurements of the scattering cross-section of a circular form and expected theoretical curve.

(figure 5(a)). The trajectories of the marble before and after the collision are traced (figure 5(b)), then the scattering angles are measured and tabulated according to a certain acceptance angle $\Delta\theta$.

Figure 6 reports the experimental scattering cross-section of a circular form of radius $R_F = 11{,}2$ cm using a marble of radius $r_M = 2.2$ cm with 88 equally spaced (0.5 cm) launches. In equations (4) and (9), we have substituted $R = \frac{R_F + r_M}{2}$, $\Omega = \Delta\theta = 0.1745$, and $n = 2R$.

With a similar procedure, the experimental cross-section of forms with different shapes, parabolic (see activity in 3.2.3 for its importance), elliptical, triangular, etc, can be measured.

3.3. Depth distribution of an element and inelastic ion energy loss

If the collision does not occur at the sample surface, the ion loses part of its energy, before hitting a nucleus. Moreover, this ion, in its back path, traverses again the layer before

emerging from the sample surface. The detected ion energy results are lower than in the case of surface scattering due to the many small interactions with the electrons of matter: the deeper the target atom, the lower the ion energy. Due to the difficulties in modeling this statistical phenomenon, the differential energy loss of ions $\frac{dE}{dx}(Z, E)$, strongly dependent on the atomic number besides the scattering angle, is evaluated experimentally for every element, where Z is the element mass, and E the ion energy. The quantity useful for RBS is the stopping cross-section, defined as the energy loss normalized by the element atomic density ρ

$$\varepsilon(Z, E) = \frac{1}{\rho}\frac{dE}{dx}(Z, E). \tag{11}$$

The stopping cross-section is not affected by the different densities of the elements, and clearly exhibits a strong increase with atomic number, with small oscillations mostly due to the difference in orbital electronic density distribution (Chu *et al* 1978).

If we consider thin surface layers, we can approximate[8] the stopping cross-section as constant like a friction parameter: at the sample surface value $\varepsilon(Z, E) \approx \varepsilon(Z, E_0)$ in the inward path, and at the value after a scattering at the surface $\varepsilon(Z, E) \approx \varepsilon(Z, K(M, \theta)E_0)$ in the outward path. In this way, the energy loss in traversing a thickness Δx is given by $\Delta E = \varepsilon(Z, E)\delta\Delta x$. In an RBS spectrum, a homogeneous layer of thickness Δx results in a nearly box-like energy band. The lower boundary is the energy $E(Z, \theta, \Delta x)$ of an ion emerging from the sample after a collision at a depth Δx and having lost an amount of energy $\Delta E_{IN} = \varepsilon(Z, E_0)\rho\Delta x$ in its inward path and $\Delta E_{OUT} = \varepsilon(Z, K(M, \theta)E_0)\rho\Delta x/|\cos\theta|$ in the outward path. The higher boundary is the energy $E(Z, \theta, 0) = K(M, \theta)E_0$ of an ion after a surface collision. The energy bandwidth of the RBS spectrum of a layer of thickness Δx turns out to be

$$
\begin{aligned}
\delta E(Z, \theta, \Delta x) &= E(Z, \theta, 0) - E(Z, \theta, \Delta x) = K(M, \theta)E_0 - (K(M, \theta)(E_0 - \Delta E_{IN}) \\
&\quad - \Delta E_{OUT}) = (K(M, \theta)\varepsilon(Z, E_0) + \varepsilon(Z, K(M, \theta)E_0)/|\cos\theta|)\rho\Delta x
\end{aligned}
\tag{12}
$$

which, under the applied approximation, proves to be proportional to $\rho\Delta x$. Note that from an RBS spectrum, as from all the other nuclear techniques, we cannot obtain direct information about the thickness Δx of a layer, but only about the product $\rho\Delta x$, i.e. the number of atoms of the element per unit area $n = \rho\Delta x$ in the layer. This means that thicknesses are measurable once the atomic densities are known, or vice versa.

3.3.1. Didactic activity: Measurement of energy loss (introductory—experimental). With the same macroscopic simulator of section 3.1.2, the role of the stopping of the impinging ion due to the crossing of matter can be evidenced. Small pieces of paper, e.g. post-its, are stuck, equally spaced, along the track. The post-it number per unit length λ represents the sample atomic density ρ in 1D, while the length L of the track segment with the post-its represents the thickness Δx of the layer. λL, i.e. the number of post-its on the track, represents, in 1D, the number of atoms of the element per unit area in the layer $n = \rho\Delta x$. After positioning a target cart of mass $M = 2.108$ kg on one side of the post-it layer, and measuring, with a sonar sensor, the velocity of the projectile cart of mass $m = 0.605$ kg entering and, after the collision, leaving the post-it segment, it is possible to evaluate the energy bandwidth δE, in analogy to equation (12), under various conditions. Figure 7 (top) shows the measurement apparatus. Figure 7 (bottom) reports the measurement of δE as a function λL (from 1–7) with constant L (60 cm). The slope of the experimental points represents the term in parenthesis of
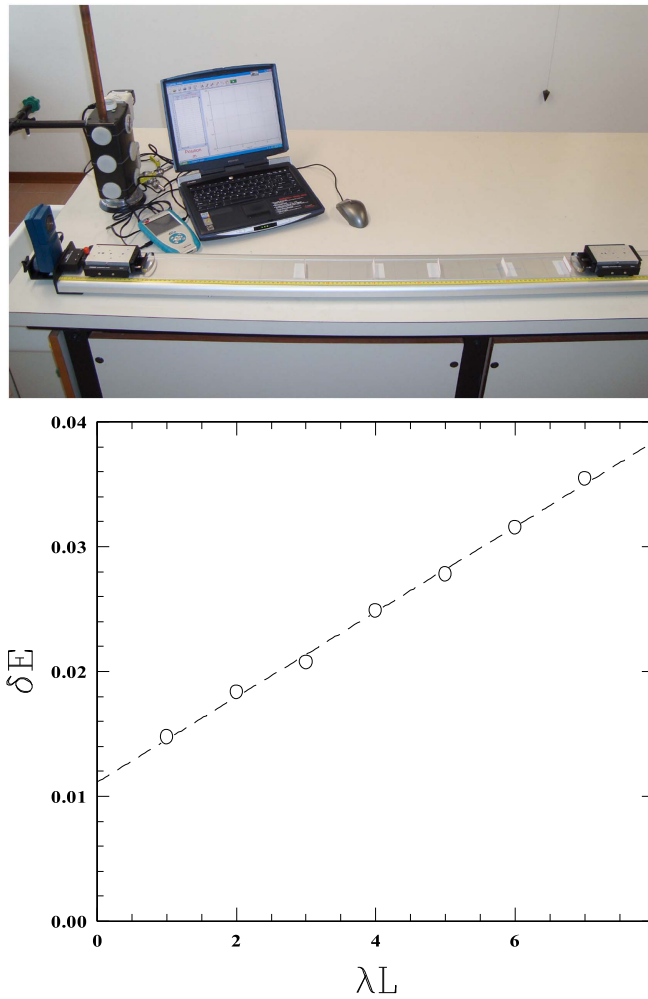
---

[8] This approximation is called surface approximation.

Figure 7. (top) Experimental setup for measurements of energy loss with track and carts. (bottom) Energy bandwidth as a function of λL ($n = \rho \Delta x$) with constant L (Δx).

equation (12). The non-zero intercept is an artifact of the experimental setup, due to the friction with the track.

The change of energy bandwidth with constant L, i.e. Δx, but with varying $L\lambda$, i.e. $n = \rho \Delta x$, allows us to recognize that, according to equation (12), with collision experiments, we cannot distinguish between thickness and atomic density of a layer.

3.4. RBS analysis

In summary, an RBS spectrum of a surface layer, with thickness Δx_S and atomic density ρ_S, of an element with atomic number Z_S and mass M_S results in a band, with the high-energy edge at $K(M, \theta)E_0$, width $\delta E(Z_S, \theta, \Delta x_S)$ (equation (12)) and normalized yield $\sigma(Z_S, \theta)\rho_S \Delta x_S$ (equation (5)) (see the contribution of Ti in figure 1). In the case of a buried layer of an element of atomic number Z_B and mass M_B, the high-energy edge is displaced at lower values than $K(M_B, \theta)E_0$ (see the Si contribution in figure 1). The energy

Table 2. Sketches of simulated RBS spectra of some sample structures. The energy positions of the single elements at the surface are marked.

| Sample structure	Simulated qualitative RBS spectrum
Thin layer of element A on a substrate of element S	
Thick layer of element A on a thin layer of element B on a substrate of element S	
Layer of element C on a substrate of element S	
Thin layer of element B on a thin layer of element A on a substrate of element S	

Table 2. (Continued.)

Sample structure	Simulated qualitative RBS spectrum
Thick layer of element B on a thin layer of element A on a substrate of element S	
Thin layer of compound AB on a substrate of element S	
Thin layer of compound AB_3 on a substrate of element S	
Thin layer of compound AS on a substrate of element S	

Table 3. Examples of sample structures, corresponding RUMP commands, and RBS simulated spectra. The expected energy positions of the single elements at the surface are marked.

Sample structure

150 nm layer of element A on 150 nm layer of element B on a substrate of element S

Beam energy 2 MeV, scattering angle 160°
RUMP commands:
reset
mev 2
theta 0
phi 20
sim layer 1 thickness 1500 A composition Zn 1/
next thickness 1500 A composition Ti 1/
next thickness 20 000 A composition Si 1/
FWHM 10
econv 3.3 100
lt 1
plot 0
element Zn element Ti element Si
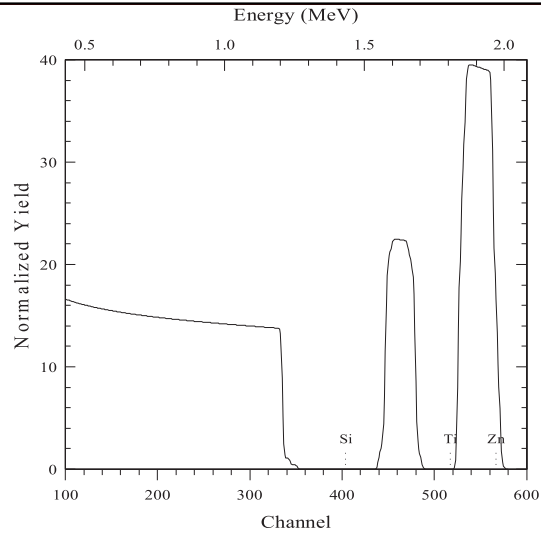
500 nm layer of compound SC$_2$ on a substrate of element S

Beam energy 2 MeV, scattering angle 160°
RUMP commands:
reset
mev 2
theta 0
phi 20
sim layer 1 thickness 5000 A composition O 2 Si 1/
next thickness 20 000 A composition Si 1/
FWHM 10
econv 3.3 100
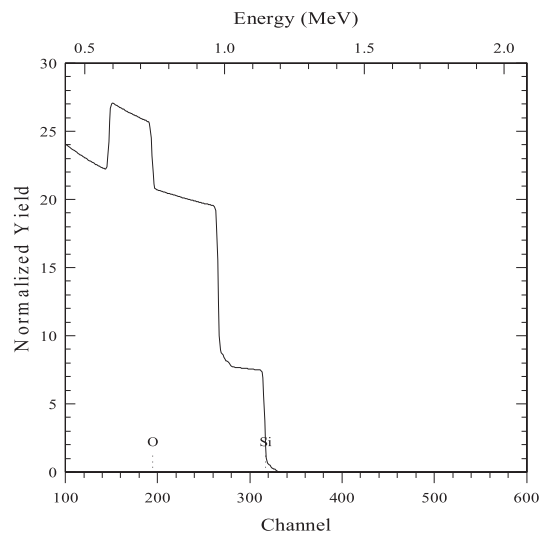lt 1
plot 0
element O element Si

Table 3. (Continued.)

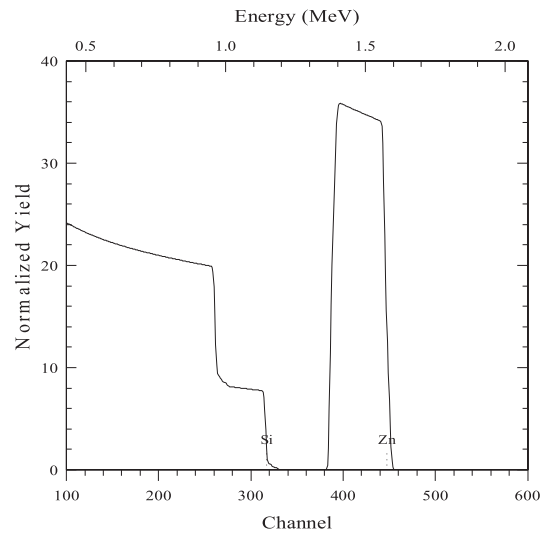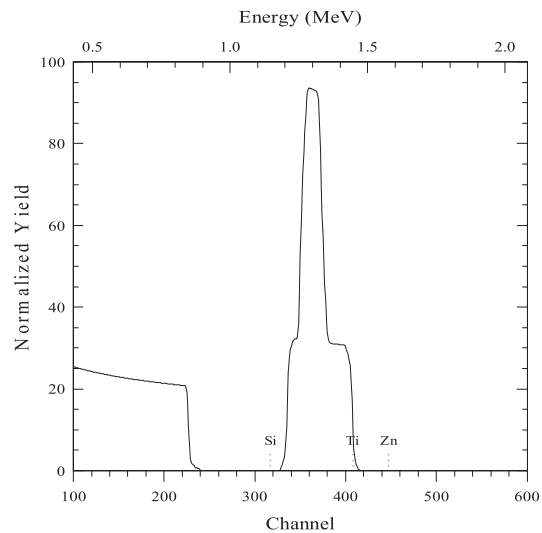| Sample structure	
300 nm layer of compound AS on a substrate of element S. Beam energy 2 MeV, scattering angle 160° RUMP commands: reset mev 2 theta 0 phi 20 sim layer 1 thickness 3000 A composition Zn 1 Si 1/ next thickness 20 000 A composition Si 1/ FWHM 10 econv 3.3 100 lt 1 plot 0 element Zn element Si	
300 nm layer of element B on 80 nm layer of element A on a substrate of element S Beam energy 2 MeV, scattering angle 160° RUMP commands: reset mev 2 theta 0 phi 20 sim layer 1 thickness 3000 A composition Ti 1/ next thickness 800 A co Zn 1/ next thickness 20 000 A co Si 1/ FWHM 10 econv 3.3 100 lt 1 plot 0 element Zn element Ti element Si	

Table 3. (Continued.)

Sample structure

150 nm layer of element A on 150 nm layer of element B on a substrate of element S

Beam energy 2 MeV, scattering angle 120°
RUMP commands:
reset
mev 2
theta 0
phi 60
sim layer 1 thickness 1500 A composition Zn 1/
ne thickness 1500 A composition Ti 1/
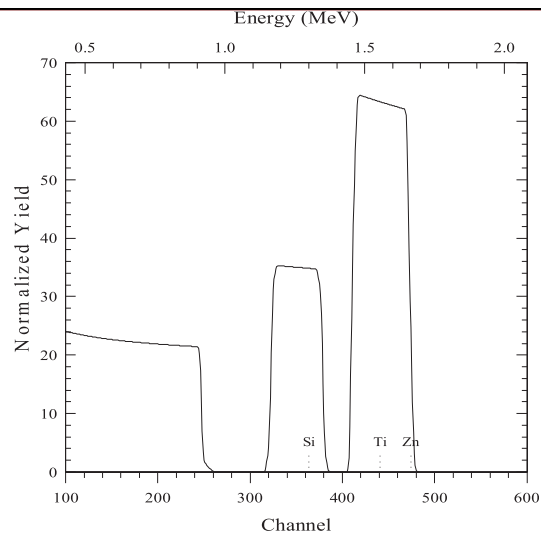next thickness 20 000 A composition Si 1/
FWHM 10
econv 3.3 100
lt 1
plot 0
element Zn element Ti element Si

150 nm layer of element A on 150 nm layer of element B on a substrate of element S

Beam energy 2.5 MeV, scattering angle 160°
RUMP commands:
reset
mev 2.5
theta 0
phi 20
sim layer 1 thickness 1500 A composition Zn 1/
next thickness 1500 A composition Ti 1/
next thickness 20 000 A composition Si 1/
FWHM 10
econv 3.3 100
lt 1
plot 0
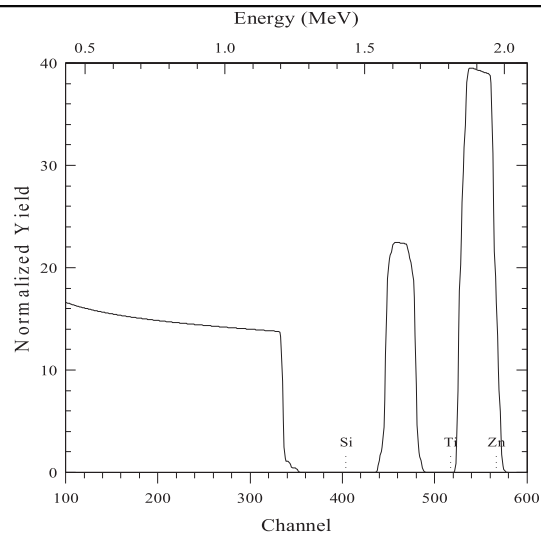element Zn element Ti element Si

17

Table 4. Blended training course for secondary school teachers.

Duration	Mode	Description	Reference
1 week	group	Reading about the basic concepts of RBS and discussion in forum both from a disciplinary and didactical point of view	sections 2 and 3
1 week	group	Analysis and discussion of RBS spectra	section 3.4.3 with spectra of table 2
1 week	individual	Design of a didactic path with the goal of allowing secondary school students to understand the basis of RBS and to interpret elementary spectra	
8 h	plenary	Conduction of laboratory activities with 50 secondary school students	See table 5

Table 5. Segment of a general physics course for undergraduate students.

Duration	Mode	Description	Reference
1.5 h	seminar	Introduction to RBS: hypotheses, main phenomena and information we can get	section 2
1.5 h	group	Experimental and theoretical activities in parallel	sections 3.1–3.3
1 h	plenary	Discussion	
30 min	seminar	Introduction to the interpretation of an RBS spectrum	section 3.4.4
1 h	group	Quantitative analysis of RBS spectra with simulation software	
1 h	plenary	Discussion	

displacement can be calculated using equation (12) with suitable substitutions $\Delta E = (K(M_B, \theta)\varepsilon(Z_S, E_0) + \varepsilon(Z_S, K(M_B, \theta)E_0)/|\cos \theta|)\rho_S \Delta x_S$. If a layer contains mixed elements or compounds, the yield of the RBS spectrum of every element of the layer will be scaled proportionally to the element fraction (equation (5)).

3.4.1. Didactic activity: qualitative simulation of RBS spectra (advanced—simulation).
Students are involved in drawing qualitative simulations of RBS spectra of given sample structures. Table 2 lists some examples of problems posed to the students and successfully solved. The masses (and the atomic numbers) of the elements A, B, C, and S are in the following order: $M_A > M_B > M_S > M_C$.

3.4.2. Didactic activity: quantitative simulation of RBS spectra (advanced—simulation).
RUMP[9] is a free package providing comprehensive analysis and simulation of RBS. Students generate RBS spectra, starting from a sample structure and composition, and see/discuss what happens by changing the element or sample structure, as well as measurement parameters (scattering angle, beam energy, etc). Initially, they reproduce some of the exercises proposed in table 2, using, for example, A = Zn, B = Ti, C = O, S = Si, then they imagine different and new sample structures (see table 3 for some key examples with RUMP commands to obtain the simulated spectra).

---

[9] RUMP (Computer Graphic Service) download page: http://genplot.com, command reference: http://genplot.com/doc/rump.htm.

Table 6. Modern physics laboratory for secondary school students.

Duration	Mode	Description	Reference
1 h	seminar	Introduction to RBS guided by concrete questions, oriented to obtain information from the spectra	sections 3.1–3.3
1 h	group	Experimental and theoretical activities in parallel	sections 3.1.1, 3.1.2, 3.2.4
40 min	plenary	Discussion of the results	
20 min	seminar	Introduction to the interpretation of an RBS spectrum	See points in 3.4.4
1 h	individual	Interpretation of RBS spectra	Spectra of table 3
2 h	plenary	Discussion of the spectra interpretations	
1 h	individual	Building of RBS spectra	Spectra of table 2
1 h	plenary	Discussion	

RUMP, like many other of this kind, besides the spectra simulations, gives numerical values of kinematic factors, scattering and stopping cross-sections of every element and of some compounds. These values can be retrieved by students and used, for example, to study the behavior of these quantities as a function of the scattering angle and of the atomic number or mass[10].

3.4.3. Didactic activity: qualitative analysis of RBS spectra (advanced, analysis). RBS spectra, no matter whether real or simulated, can be given to the students so that they can guess and discuss the structure and composition of the sample on the basis of their knowledge (see section 2). Some real RBS spectra are supplied with this paper (together with the simulation macros for RUMP), and others can be found on the Internet or in journal articles. In the absence of real data, the teacher can generate incognito RBS spectra through RUMP or use those of table 3.

3.4.4. Didactic activity: quantitative analysis of RBS spectra (advanced, analysis). Using the same spectra, students, equipped with simulation software such as RUMP, experience the thrill of performing actual sample analyses.

The steps for a spectrum analysis we set up according to research-based intervention modules we experimented is organized in the following steps.

- *Determine the element(s) of the surface layer.*
  Proceeding from higher to lower energies, guess a possible element at the sample surface. If the element peak does not show the expected yield, it is possible that a compound surface layer is present. In this case, search for the other component(s) and determine the atomic composition of the surface layer.
- *Calculate the thickness of the surface layer.*
  Determine the thickness of the surface layer that accounts for the width(s) and the height(s) of the surface layer peak(s).
- *With analogous procedure, determine elements, atomic compositions and thicknesses of the underlying layers.*
- *Determine the substrate composition.*

[10] Example of meaningful 3D graphs are reported in (Chu et al 1978).

4. Research-based path proposal

The activities presented here are the follow-up of the research-based intervention modules we experimented in IDIFO summer schools for teachers in 2014 and for talented secondary school students from 2007–2016 (Michelini and Santi 2008, Corni 2008, 2010, Michelini 2010b, Mossenta 2010, 2012, Battaglia *et al* 2011). In tables 4, 5, and 6, we outline possible didactic sequences suitable for a training course for secondary school teachers, a general physics course for undergraduate students, and a laboratory for secondary school students, respectively.

5. Summary

We have presented a variety of activities about RBS suitable for all kinds of student inclination and laboratory equipment. Some of them are introductory activities about the single phenomena of RBS, while others are advanced activities about the RBS technique itself. We have also exemplified how these activities can be composed into didactic paths, suitable for secondary school teachers, undergraduate and secondary school students.

The didactic proposal offers the opportunity for students to see how the historical Rutherford experiment leads to the development of a modern analysis technique such as RBS, based on classical physics and relying on the fundamental principles of conservation. Elastic nuclear collision, Coulomb scattering, and ion stopping are introduced through inquiry-type questions aimed at obtaining information about the composition and structure of a sample. Elastic nuclear collision leads to the definition of the kinematic factor. Mathematical calculation of the kinematic fraction makes the students study its behavior analytically, while track and carts allow them to measure the kinematic factor as a function of the target mass. The Coulomb scattering leads to the notion of scattering cross-section. The mathematical evaluation of the Rutherford scattering cross-section is an opportunity for students to discuss its analytical form together with the adoptable approximations. 2D reduction allows them to better visualize the cross-section analytical shape and to perform statistical measurements. Finally, ion stopping leads to the notion of stopping cross-section. Experiments with track and carts make the students reflect on the meaning of the energy bandwidth of the RBS spectrum of an element layer.

The activities about RBS challenge the students to engage their knowledge about the various phenomena to interpret or build RBS spectra. The availability of simulators, e.g. RUMP, allows the students to build and discuss spectra, starting from hypothetical sample structures and changing the parameters. Qualitative and quantitative didactic simulation activities are suggested. The students can also experience the thrill of performing real sample analyses. We propose activities of qualitative analysis where students interpret the RBS spectra by deduction from the equations, as well as activities of quantitative analysis following a fitting procedure with simulated data. Experimental RBS spectra are supplied with this paper, together with the RUMP macros giving the optimized simulations.

The experimentations, which have been performed during the last ten years in Italy, show quick and good responses from the students and teachers.

Acknowledgments

ORCID iDs

Federico Corni ⓘ https://orcid.org/0000-0003-1226-1585

References

Anderson T and Shattuck J 2012 Design-based research: a decade of progress in education research? *Educ. Res.* **41** 16–25

Battaglia R, Cazzaniga L, Corni F, Ambrosis A, De, Fazio C, Giliberti M and … Stefanel A 2011 Master IDIFO (Innovazione Didattica In Fisica e Orientamento): a community of Italian physics education researchers and teachers as a model for a research based in-service teacher development in modern physics *Physics Community and Cooperation* ed D Raine, C Hurkett and L Rogers (Leicester: University of Leicester) pp 97–136

Chadwick J 1913 The excitation of gamma rays by alpha rays *Philos. Mag. Series* **6** 193–7

Chadwick J and Bieler E S 1921 The collisions of alpha particles with hydrogen nuclei *Philos. Mag. Series* **6** 923–40

Chong F and Andrews R J 1993 Rutherford scattering made simple by using complex numbers *Eur. J. Phys.* **14** 245–7

Chu W-K, Mayer J W and Nicolet M-A 1978 *Backscattering Spectrometry* (San Diego, CA: Academic)

Corni F 2008 A proposal about Rutherford Backscattering Spectrometry for a second level master in physics education *Frontiers of Physics Education—Selected Contributions* (Rijeka: R. Jurdana-Sepic) M.Zuvic-Butorac, Golden section pp 132–6

Corni F 2010 RBS-Rutherford Backscattering Spectrometry: cimentarsi in una tecnica di analisi della ricerca nella fisica dei solidi ed M Michelini *Fisica Moderna per la Scuola* (Udine: Università degli Studi di Udine) pp 109–20

Corni F, Michelini M, Santi L, Soramel F and Stefanel A 1996 The concept of the cross section ed M Michelini *Teaching the Science of Condensed Matter and New Materials* (Udine: Forum) pp 192–8

DBRC 2003 Design-based research: an emerging paradigm for educational inquiry *Educ. Res.* **32** 5–8

Duit R, Gropengiesser H and Kattmann U 2005 Toward science education research: the model of educational reconstruction ed H E Fisher *Developing Standard in RSE* (London: Taylor & Francis)

Eaton T W and Cheetham D 1973 A novel design of Rutherford scattering apparatus *Phys. Educ.* **8** 97–101

Feldman L C and Mayer J W 1982 *Materials Analysis by Ion Channelling* (New York: Academic)

Feldman L C and Mayer J W 1986 *Fundamentals of Surface and Thin Film Analysis* (New York: North-Holland)

Gauthier N 2000 Simple quantum calculation of the Rutherford cross section *Eur. J. Phys.* **21** L17–8

Grober S, Vetter M, Eckert B and Jodl H-J 2010 Experimenting from a distance in the case of Rutherford scattering *Eur. J. Phys. (UK)* **31** 727–33

Jeynes C 2017 RBS as a new primary direct reference method for measuring quantity of material *Nucl. Instr. Meth. Phys. Res. section B: Beam Interactions with Materials and Atoms* **406** 30–1 part A

Jeynes C and Colaux J L 2016 Thin film depth profiling by ion beam analysis *Analyst* **141** 5944–85

Lee P M, Montagu-Pollock H M and Perkins A 1968 A Rutherford alpha particle scattering analogue *Phys. Educ.* **3** 211–2

Lijnse P L 1995 'Developmental research' as a way to an empirically based 'didactical structure' of science *Sci. Educ.* **79** 189–99

Michelini M 2010a Building bridges between common sense ideas and a physics description of phenomena *New Trends in Science and Technology Education* ed L Menabue and G Santoro (Bologna: Clueb) pp 257–74

Michelini M 2010b *Fisica Moderna per la Scuola. Materiali, aspetti e proposte per l'innovazione didattica e l'orientamento* ed M Michelini (Udine: Università degli Studi di Udine) Retrieved from (http://fisica.uniud.it/URDF/laurea/materiali/pdf/fisica_moderna.pdf)

Michelini M and Santi L 2008 Master IDIFO for in-service teacher training in modern physics *Frontiers of Fundamental and Computational Physics—FFP9* ed B Sidharth, F Honsell, O Mansutti, K Sreenivasan and A DeAngelis (Melville, NY: American Institute of Physics) pp 253–4

Michelini M, Santi L and Stefanel A 2016 Research based proposals to build modern physics way of thinking in secondary students. In K. A & T. T (Eds.) *Teaching Physics Innovatively* (Budapest: University of Budapest) pp 331–50

Mossenta A 2010 La tecnica RBS in classe: un ponte tra la ricerca e la scuola per insegnare alcune delle basi della fisica *Comunicare Fisica e altre Scienze* vol II (Frascati: Scienza Aperta)

Mossenta A 2012 Interpretare le interazioni elettrostatiche: dal processo di ricerca alla Rutherford Backscattering Spectrometry *PhD Thesis* University of Udine

Rutherford E 1911 The scattering of α and β particles by matter and the structure of the atom *Phil. Mag.* **6** 669–88

Rutherford E 2012 The scattering of α and β particles by matter and the structure of the atom *Phil. Mag.* **92** 379–98

Rutherford E and Chadwick J 1922 The disintegration of elements by α particles *Philos. Mag. Series* **6** 417–32

Wicher E R 1965 Elementary Rutherford scattering simulator *Am. J. Phys.* **33** 635–6